

# Prediction of wall shear stress in the arteries with myocardial bridge by neural networks

Dalibor Nikolić<sup>2\*</sup>, Igor Saveljić<sup>1,2</sup>, Miloš Radović<sup>1,2</sup>, Srđan Aleksandrić<sup>3</sup>, Miloje Tomašević<sup>3,4</sup>, Vesna Ranković<sup>1</sup>, Nenad Filipović<sup>1,2</sup>,

<sup>1</sup>Faculty of Engineering University of Kragujevac, Sestre Janjic 6, 34000 Kragujevac, Serbia

<sup>2</sup>Bioengineering Research and Development Center, Prvoslava Stojanovica 6, 34000 Kragujevac, Serbia

<sup>3</sup>Clinic of Cardiology, Clinical center of Serbia, Visegradska 26, 11000 Belgrade, Serbia

<sup>4</sup>Faculty of Medical Sciences, University of Kragujevac, Svetozara Markovića 69, 34000 Kragujevac, Serbia

markovac85@kg.ac.rs

isaveljic@kg.ac.rs

mradovic@kg.ac.rs

srdjanaleksandric@gmail.com

tomasevicmiloje@gmail.com

vesnar@kg.ac.rs

fica@kg.ac.rs

**Abstract**— Coronary arteries and their major branches, which supply oxygenated and nutrient filled blood to the heart muscle (myocardium), lie on the surface of the heart, in the subepicardial space, between visceral pericardium (epicardium) and myocardium. Sometimes, a shorter or longer segment of the epicardial coronary artery or its branch is covered by a band of heart muscle that lies on top of it. This band of muscle is called a “bridge” and the intramural segment of coronary artery a “tunneled artery”.

**Myocardial bridging (MB)** is a congenital coronary anomaly defined as a segment of a major epicardial coronary artery that runs intramurally through the myocardium beneath the muscle bridge.

**It is very important to find the most efficient method for determining shear stress in the coronary arteries with myocardial bridge.**

**The procedure for calculating shear stress in MB arteries using neural networks trained with results from finite elements method will be explained in this paper.**

## I. INTRODUCTION

The value of shear stress in the artery with MB is very important for the medical doctors. Low and oscillatory shear stress, with a low time-averaged values (<1.5 N/m<sup>2</sup>), lead to alterations in the expression of vasoactive agents, such as endothelial nitric oxide synthase (eNOS), endothelin-1 (ET-1), angiotensin-converting enzyme (ACE) and growth-promoting and prothrombotic phenotype, ultimately acquiring a predisposition to atherosclerosis [1, 3, 4, 5]. On the other hand, the normal shear stress, with a positive time-average ranging between 1.5 N/m<sup>2</sup> and 7.0 N/m<sup>2</sup>, increases the production of nitric oxide (NO) in endothelial cells and downregulates the expression of proatherogenic molecules, related to an atheroprotective effect [1,3,4,5]. In addition, scanning electron microscopy reveals the changes in the shape of the endothelial cells in LAD intima from flat and polygonal in the segment proximal to the MB to helical, spindle-shaped under the MB [2,6,7].

Since it is not possible to measure shear stress in the artery with myocardial bridge, it is very important to find the method for calculating this value.

One of most effective methods is FEM (Finite Element Method). Since it is a very complicated and slow process of mesh generating and solving which requests a very high computational power, we try to find some faster and easier methods to use, such as neural networks.

## II. METHODS AND MATERIALS

### A. Developing geometrical FE model Artery with MB

FE model of artery with MB is created in our software for generating and meshing finite element models. After meshing, the application automatically runs the FE solver, waiting for the results and then imports them and creates a file for training neural networks. Application block diagram is presented in the Figure 1. [13].

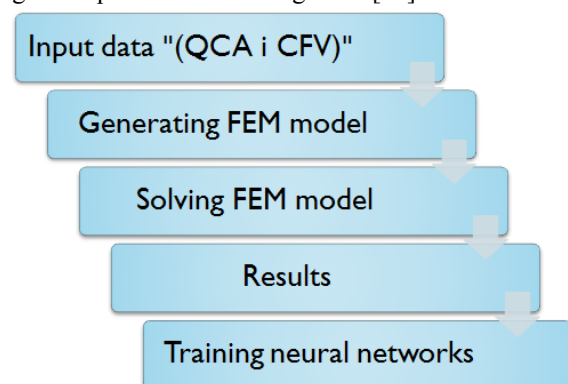


Figure 1. Block diagram

Segmentation of CT images is the best method to create the geometry of certain organ, but MB is very rare disease and in the medical practice, it is detected by angiography. For this reason, the software application is developed to generate the geometry from QCA measurements data from angiographic images.

Time interval - the end of systole			
Length MB	The diameter of the artery in the MB	The diameter of the artery in front of the MB	The diameter of the artery behind the MB
Time interval - early diastole			
Length MB	The diameter of the artery in the MB	The diameter of the artery in front of the MB	The diameter of the artery behind the MB
Time interval - mid-diastolic			
Length MB	The diameter of the artery in the MB	The diameter of the artery in front of the MB	The diameter of the artery behind the MB
Time interval - end-diastolic			
Length MB	The diameter of the artery in the MB	The diameter of the artery in front of the MB	The diameter of the artery behind the MB
Inlet velocity			

Figure 2. Input data from QCA

Additionally, the software automatically generates four geometrically different meshes for each of the measured periods of a heart cycle. (Figure 2). Based on these four meshes, the software interpolates the shape of the mesh model throughout the cardiac cycle. This mesh movement is very important for accurate computation of blood flow through MB.

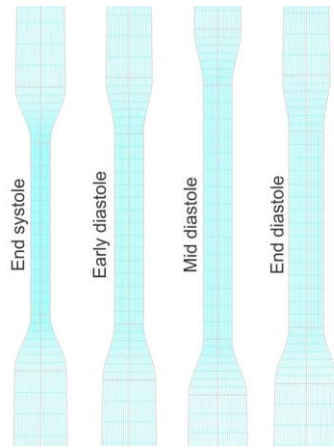


Figure 3. Generated FE 2D model meshes during 4 periods of a heart cycle

**B. FEM mathematical method**

A finite element model of the bridge was employed. Flow in the coronary artery is a complex, time-dependent, three-dimensional flow. The time-dependent and full three-dimensional Navier-Stokes equations have to be solved. A finite element mesh with 8247 2D 4 node axisymmetric finite elements was generated using an automatic mesh generator as it is presented in the Figure 3. The mesh independence was reached at 6530 to 25375 finite elements.

The three-dimensional flow of a viscous incompressible fluid considered here is governed by the Navier- Stokes equations and continuity equation that can be written as

$$\rho \left( \frac{\partial v_i}{\partial t} + v_j \frac{\partial v_i}{\partial x_j} \right) = -\frac{\partial p}{\partial x_i} + \mu \left( \frac{\partial^2 v_i}{\partial x_j \partial x_j} + \frac{\partial^2 v_j}{\partial x_i \partial x_i} \right) \quad (1)$$

$$\frac{\partial v_i}{\partial x_i} = 0 \quad (2)$$

where  $v_i$  is the blood velocity in direction  $x_i$ ,  $\rho$  is the fluid density,  $p$  is pressure,  $\mu$  is the dynamic viscosity; and summation is assumed on the repeated (dummy) indices,  $i,j=1,2,3$ . The first equation represents balance of linear momentum, while the equation (2) expresses incompressibility condition.

Each waveform of and pulsatile flow was discretized into 500 uniformly spaced time steps. In the analysis, it was considered that the convergence was reached when the maximum absolute change in the nondimensional velocity between the respective times in two adjacent cycles was less than  $10^{-3}$ .

The code was validated using the analytical solution for shear stress and the velocities through curve tube [8]. The pressure is eliminated at the element level through the static condensation.

A standard Petrov-Galerkin upwind stabilization technique was used for Re number [8].

In addition to the velocity field, the wall shear stress computation was performed. The mean shear stress  $\tau_{mean}$  within a time interval  $T$  is calculated as [9]

$$\tau_{mean} = \left| \frac{1}{T} \int_0^T t_s dt \right| \quad (3)$$

where  $t_s$  is the surface traction vector. Another scalar quantity is a time-averaged magnitude of the surface traction vector, calculated as

$$\tau_{mag} = \frac{1}{T} \int_0^T |t_s| dt \quad (4)$$

Also, a very important scalar in the quantification of unsteady blood flow is the oscillatory shear index (OSI) defined as [9]

$$OSI = \frac{1}{2} \left( 1 - \frac{\tau_{mean}}{\tau_{mag}} \right) \quad (5)$$

$$Re sT = ((1 - 2 \cdot OSI) \cdot \tau_{mag})^{-1} \quad (6)$$

In order to make mesh moving algorithm we implemented ALE (Arbitrary Lagrangian Eulerian) formulation for fluid dynamics [10]. The governing equations, which include the Navier-Stokes equations of balance of linear momentum and the continuity equation, can be written in the ALE formulation as [10].

$$\rho [v_i^* + (v_j - v_j^m) v_{i,j}] = -p_{,i} + \mu v_{i,jj} + f_i^B \quad (7)$$

$$v_{i,i} = 0 \quad (8)$$

where  $v_i$  and  $v_i^m$  are the velocity components of a generic fluid particle and of the point on the moving mesh occupied by the fluid particle, respectively;  $\rho$  is fluid density,  $p$  is fluid pressure,  $\mu$  is dynamic viscosity, and  $f_i^B$  are the body force components. The symbol “ $*$ ” denotes the mesh-referential time derivative, i.e. the time derivative at a considered point on the mesh,

$$(\ )^* = \frac{\partial(\ )}{\partial t} \Big|_{\xi_i=const} \quad (9)$$

and the symbol “ $_{,i}$ ” denotes partial derivative, i.e.

$$(\ )_{,i} = \frac{\partial(\ )}{\partial x_i} \quad (10)$$

We use  $x_i$  and  $\xi_i$  as Cartesian coordinates of a generic particle in space and of the corresponding point on the mesh, respectively. The repeated index means summation, from 1 to 3, i.e.  $j=1,2,3$  in Eq. (7), and  $i=1,2,3$  in Eq. (8). In deriving Eq. (7) we used the following expression for the material derivative (corresponding to a fixed material point)  $D(\rho v_i)/Dt$ ,

$$\frac{D(\rho v_i)}{Dt} = \frac{\partial(\rho v_i)}{\partial t} \Big|_{\xi} + (v_j - v_j^m) \frac{\partial(\rho v_i)}{\partial x_j} \quad (11)$$

The derivatives on the right-hand side correspond to a generic point on the mesh, with the mesh-referential derivative and the convective term.

### C. Neural networks

The results from FEM models are used for training neural networks. For this research we made calculation for 12 different patients with MB. In order to train the neural networks, a large number of patients were required. For these purposes, input data for 2000 patients were randomly generated, based on the data from real patients with deviation 30%.

### D. Neural network model

A graphical structure of neural network used for the prediction of the shear stress on arteries with MB is presented in the Figure 4.

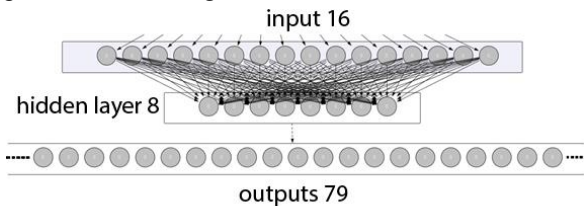


Figure 4. Graphical representation of neural network

### E. Software solution for neural networks

To generate and training (Figure 5) neural network is used a software package MATLAB v.13

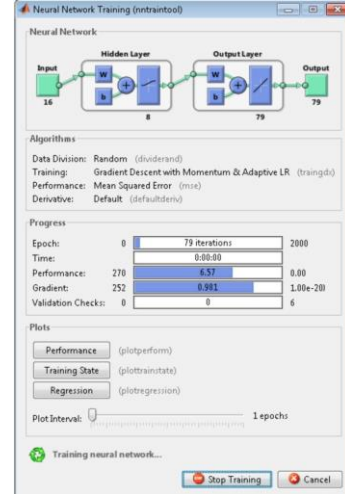


Figure 5. MATLAB Neural network training

### F. Methodology neural networks

The traditional form of the back propagation algorithm has a problem with the local minimums and slow convergence. In order to overcome these problems, numerous variations of this algorithm have been developed [14]. For prediction of WSS, REST and OSI the multilayer perceptron neural network was used. This network was trained with back propagation algorithm. The adaptation of weight coefficient

$$w_{i,j(l)}(t+1) = w_{i,j(l)}(t) + \Delta w_{i,j(l)}(t+1)$$

$$w_{i,j(l)}(t+1) = \eta \alpha \frac{\partial E_k}{\partial w_{i,j(l)}} + \alpha \Delta w_{i,j(l)}(t) \quad (12)$$

The learning speed  $\eta$  in the equation (12) is variable. In every epoch, if the criteria function is decreased towards the aim, the learning speed is increased for factor  $\eta_{inc}$ . The values of the parameters  $\alpha$ ,  $\eta_{inc}$ ,  $\eta_{dec}$  and  $max_{inc}$  used for solving the problem are presented in Table I.

TABLE I.  
BACK PROPAGATION ALGORITHM PARAMETER VALUES

$\alpha$	$\eta_{inc}$	$\eta_{dec}$	$max_{inc}$
0.9	1.05	0.7	1.04

The criterion for learning stopping is defined as 2000 epochs.

### III. RESULTS

The neural network was tested by the *10-fold cross validation* algorithm and by calculating relative mean squared error - RMSE:

$$RMSE = \frac{\sum_{i=1}^N \sum_{j=1}^S (y_i(j) - \hat{y}_i(j))^2}{\sum_{i=1}^N \sum_{j=1}^S (y_i(j) - \bar{y}(j))^2} \quad (15)$$

where  $N$  is the total number of the examples (2000),  $s$  is the total number of the outputs (79),  $y_i(j)$  is the real value of the  $j$ -th output,  $i$ -th example,  $\bar{y}(j)$  is the mean value of the  $j$ -th output, and  $\hat{y}_i(j)$  is the neural network prediction of the  $j$ -th output,  $i$ -th example.

RMSE values obtained by neural network testing are presented in Table II.

TABLE II.  
RMSE VALUES OBTAINED BY TESTING OF THE NEURAL NETWORK

Model	RMSE
WSS	0.0964
ResT	0.2873
OSI	0.1507

The value of RMSE which is lower than 1.0 shows that the model is usable (it has a lower error than non-intelligent model) [15]. From Table II, it can be concluded that the neural network has presented a high potential for the prediction of WSS, ResT, OSI.

### IV. CONCLUSION

The advantage of neural networks lies in the fact that when one is trained, based on several input parameters, it provides very accurate results in just a few seconds, which is crucial in the clinical practice. However, the biggest disadvantage is that for training the network we must use the results previously obtained from the methods such as finite element method provided by numerous simulations.

This process of preparation of the results for neural networks training is very slow and it requires a high computing power to solve all of the FEM models and a trained person with the experience in FEM method.

### V. ACKNOWLEDGMENT

This work was supported in part by grants from Serbian Ministry of Education and Science III41007, ON174028.

### REFERENCES

- [1] JR. Alegria, J. Herrmann, DR Jr Holmes, A. Lerman, SR. Charanjit. Myocardial bridging. *Eur Heart J*, 2005, 26:1159–1168.
- [2] S. Möhlenkamp, W. Hort, J. Ge, R. Erbel. Update on Myocardial Bridging. *Circulation*, 2002, 106:2616-2622
- [3] YS. Chatzizisis, GD. Giannoglou, Myocardial bridges are free from atherosclerosis: Overview of the underlying mechanisms. *Can J Cardiol*, 2009, 25:219-222.
- [4] AM. Malek, SL. Alper, S. Izumo, Hemodynamic shear stress and its role in atherosclerosis. *JAMA* 1999, 282:2035-42.
- [5] YS. Chatzizisis, AU. Coskun, M. Jonas, ER. Edelman, CL. Feldman, PH. Stone, Role of endothelial shear stress in the natural history of coronary atherosclerosis and vascular remodeling: Molecular, cellular and vascular behavior. *J Am Coll Cardiol*, 2007, 49:2379-93.
- [6] Y. Ishikawa, Y. Kawawa, E. Kohda, K. Shimada, T. Ishii. Significance of the anatomical properties of a myocardial bridge in coronary heart disease. *Circ J*, 2011, 75:1559-1566.
- [7] T. Ishii, Y. Hosoda, T. Osaka, T. Imai, H. Shimada, A. Takami, H. Yamada. The significance of myocardial bridge upon atherosclerosis in the left anterior descending coronary artery. *J Pathol*, 1986, 148:279–291.
- [8] N. Filipovic, M. Kojic, M. Ivanovic, B. Stojanovic, L. Otasevic, V. Rankovic, MedCFD, Specialized CFD software for simulation of blood flow through arteries, (University of Kragujevac, 34000 Kragujevac, Serbia, 2006)
- [9] C.A. Taylor, T.J.R Hughes and C.K. Zarins, Finite element modeling of blood flow in arteries, *Comput. Meths. Appl. Mech. Engrg* 158, 1999, 155-196.
- [10] N. Filipovic, S. Mijailovic, A. Tsuda, M. Kojic, An implicit algorithm within the Arbitrary Lagrangian-Eulerian formulation for solving incompressible fluid flow with large boundary motions, *Comp. Meth. Appl. Mech. Eng* 195, 2006, 6347-6361.
- [11] J. Ge, R. Erbel, H.J. Rupprecht, L. Koch, P. Kearney, G. Gorge, M. Haude, J. Meyer, Comparison of intravascular ultrasound and angiography in the assessment of myocardial bridging. *Circulation* 89, 1994, 1725–1732.
- [12] A.M. Malek, S.L. Alper, S. Izumo, Hemodynamic shear stress and its role in atherosclerosis, *JAMA* 282, 1999, 2035-2042.
- [13] D. Nikolić, M. Radović, S. Aleksandrić, M. Tomašević, N. Filipović, Prediction of coronary plaque location on arteries having myocardial bridge, using finite element models, *Computer Methods and Programs in Biomedicine*, Vol. 117, Issue 2, 2014, pp. 137-144
- [14] M.B. Hudson, M. T. Hagan, H. B. Demuth, *Neural Network Toolbox User's Guide*, The MathWorks, Inc, [http://www.mathworks.com/help/pdf\\_doc/nnet/nnet\\_ug.pdf](http://www.mathworks.com/help/pdf_doc/nnet/nnet_ug.pdf)
- [15] I. Kononenko, M. Kukar, *Machine learning and data mining*, Horwood Publishing Chichester, UK, 2007.